Using a Coupled Lake Model with WRF for Dynamical Downscaling

Megan S. Mallard, Christopher G. Nolte, O. Russell Bullock,
Tanya L. Spero
National Exposure Research Laboratory, U.S. Environmental Protection Agency,
Research Triangle Park, North Carolina

Jonathan Gula
Institute of Geophysics and Planetary Physics,
University of California, Los Angeles, Los Angeles, California

May 19, 2014
Submitted to the Journal of Geophysical Research

Corresponding author: Megan Mallard, U.S. EPA, Mail Drop E243-01, 109 T.W. Alexander Dr., Research Triangle Park, NC 27711. (MeganSMallard@gmail.com)

Key Points

1.) Unrealistic lake temperatures and ice result when interpolating from global data

2.) WRF coupled with the FLake model improves Great Lakes temperatures and ice cover

3.) Positive precipitation bias increases despite better representation of lakes

Abstract

The Weather Research and Forecasting (WRF) model is used to downscale a coarse reanalysis (National Centers for Environmental Prediction–Department of Energy Atmospheric Model Intercomparison Project reanalysis, hereafter R2) as a proxy for a global climate model (GCM) to examine the consequences of using different methods for setting lake temperatures and ice on predicted 2-m temperature and precipitation in the Great Lakes region. A control simulation is performed where lake surface temperatures and ice coverage are interpolated from the GCM-proxy. Because the R2 represents the five Great Lakes with only three grid points, ice formation is poorly represented, with large, deep lakes freezing abruptly. Unrealistic temperature gradients appear in areas where the coarse scale fields have no inland water points nearby and lake temperatures on the finer grid are set using oceanic points from the GCM-proxy. Using WRF coupled with the Freshwater Lake (FLake) model reduces errors in lake temperatures and significantly improves the timing and extent of ice coverage. Overall, WRF-FLake increases the accuracy of 2-m temperature compared to the control simulation where lake variables are interpolated from R2. However, the decreased error in FLake-simulated lake temperatures exacerbates an existing wet bias in monthly precipitation relative to the control run because the erroneously cool lake temperatures interpolated from R2 in the control run tend to suppress over-active precipitation.

1. **Introduction**

When developing a methodology to downscale global climate model (GCM) projections to finer-scale regional climate model (RCM) simulations, a number of challenging issues must be considered, including the choice of appropriate physics parameterizations, the placement of lateral boundaries, and whether to constrain the RCM by using nudging in the domain interior. However, when downscaling a GCM using an RCM with no oceanic component, it is usually assumed that surface temperatures from the GCM are adequate to provide lower boundary conditions over water points in the RCM. In the standard configuration of the Weather Research and Forecasting (WRF) model, lake surface temperatures (LSTs) are interpolated from the sea surface temperature (SST) field in the input data. However, SST datasets provided by typically coarse GCMs do not resolve inland lakes well, if at all. If an inland water point exists on the finer WRF grid for which no water points are proximate in the GCM, the LST is instead set from the SST of the nearest water point in the GCM, resulting in lake temperatures that are frequently erroneous. Although this problem could be addressed by using an exogenous SST dataset with resolution sufficient to satisfactorily represent inland lakes, it is desirable to rely only on the GCM for input data when using WRF as an RCM to simulate future changes in regional climate.

A number of studies have shown that the Laurentian Great Lakes have a significant influence on the surrounding region, affecting precipitation, temperature, the intensity of passing cyclones and anticyclones, water vapor, cloud coverage, the placement of the jet stream and other important aspects of regional climate [e.g., Wilson, 1977; Bates et al., 1993; Lofgren, 1997; Notaro et al., 2013]. Notaro et al. [2013] conducted a decadal modeling study over the Great Lakes basin using an idealized simulation in which the lakes were replaced with field and forest land cover types, and this run was compared with a simulation containing the lakes. They found that the presence of the Great Lakes suppressed variability of the 2-m temperature at diurnal and seasonal timescales, as was also concluded by Bates et al. [1993]. The effect on precipitation varied seasonally, enhancing (suppressing) precipitation during September to March (April to August) when the greater thermal inertia of the lakes has the effect of decreasing (increasing) stability because water temperatures are warmer (cooler) than temperatures in the overlying atmosphere [Notaro et al., 2013]. Wilson [1977] found that differences between 850-hPa temperatures and LSTs in excess of 7 ^{o}C result in a substantial increase in downwind precipitation, suggesting that relatively small errors in LSTs can affect precipitation amounts. The influence of erroneous LSTs was studied by Zhao et al. [2012]. They conducted 5-year RCM simulations in the Great Lakes basin where WRF was driven with high-resolution satellite-derived LSTs and lake ice coverage, and compared this to a simulation driven with a lower-resolution reanalysis product. Lake-averaged monthly temperatures in the higher-resolution LST dataset differed from the analyzed temperatures by as much as 8 ^{o}C, and using finer satellite-derived LSTs significantly reduced erroneous winter precipitation.

Wright et al. [2013] conducted a case study of lake-effect snow in the Great Lakes region and assessed the impact of both ice and lake temperatures by comparing a control WRF simulation using realistic ice and LSTs with idealized runs that featured either complete coverage or no ice cover, as well as a simulation where LSTs were uniformly increased by 3 K. They found that the placement of ice suppressed the formation of lake-effect snow, as expected since increased ice cover and thickness had been shown to decrease latent and sensible heat fluxes (e.g., Gerbush et al., 2008; Zulauf and Krueger, 2003). Wright et al. [2013] also showed that additional warming imposed on LSTs increased the intensity and spatial coverage of snowfall. Overall, past studies conclude that the representation of the lake state in regional climate simulations can strongly affect surface temperatures and precipitation in the surrounding region.

Austin and Colman [2007] discussed the non-linearity of the effects of climate change on the Great Lakes. They examined observational records from Lake Superior for a 28-year period and showed an increased warming trend over a multi-decadal period relative to inland temperatures due to declining ice coverage and earlier onset of the summer stratification of lake temperatures. Their findings corroborate other observational studies that link multi-decadal warming trends in lake temperatures to increased lake-effect precipitation [Burnett et al., 2003; Kunkel et al., 2009] and others that find long-term decreasing trends in the duration of ice coverage in the Great Lakes [Assel and Robertson, 1995] and in northern hemispheric lakes and rivers [Magnuson, 2000]. Notaro et al. [2013] speculated that this enhanced warming of lake temperatures could lessen the springtime stabilizing influence of the Great Lakes. Lakes are an interactive component of the climate system, and this aspect of regional climate change presents a challenge to RCMs that rely on prescribed water temperatures. Wright et al. [2013] cite accurate predictions of the timing and extent of lake ice formation as critical aspects of predicting changes in lake-effect precipitation in future climates. If the warming of lake temperatures and the associated effects on ice formation are not captured by the RCM, predictions of lake-effect precipitation and inland temperatures will be adversely affected.

The overall purpose of this line of research is to establish a downscaling method in order to equip environmental managers and decision makers with tools and data to inform decisions related to adapting to and mitigating the potential impacts of regional climate change on air quality, ecosystems, and human health. One issue that has emerged in using WRF to downscale coarse-scale global climate fields is the representation of the LSTS and ice cover, particularly for lakes that are either poorly resolved or not resolved by the global fields. This study examines the methods by which LSTs and ice concentration are set in WRF within a downscaling configuration. In addition to outlining the options within the existing model capability, a modified version of WRF that is coupled to the Freshwater Lake (FLake) model is also used. The resulting ice coverage and LSTs are compared with observations and the effects on commonly used surface variables from the RCM (2-m temperature and precipitation) are examined. This study addresses whether the existing options for setting lake temperatures and ice coverage negatively affect the simulation of surface variables by WRF and whether WRF-FLake improves their representation.

2. Methods

a.) Downscaling configuration

Otte et al. [2012] described a series of regional climate simulations, performed with 108- and 36-km nested domains for 1988-2007, in which the National Centers for Environmental Prediction (NCEP)–Department of Energy Atmospheric Model Intercomparison Project (AMIP-II) reanalysis [Kanamitsu et al., 2002] (hereafter R2) was used as a proxy for a similarly coarse GCM. While it is recognized that several GCMs operate at finer resolution than the R2 (T62, $1.875° \times 1.875°$ at the equator), the resolution of this dataset is comparable to several presently used GCMs. Sillmann et al. [2013; their Supplemental Table 1] lists the spectral resolution of 15

GCMs used in the Intergovernmental Panel on Climate Change (IPCC) Fifth Assessment Report (AR5). Nine of them have spectral resolution equivalent to or coarser than T63.

Overall, the regional climatology and interannual variability simulated by the downscaled runs in Otte et al. [2012] were found to be realistic. Bullock et al. [2014] described simulations where a 12-km nest was added to the downscaling configuration of this prior study (see their Fig. 1), with focus on the sensitivity of the 12-km runs to physics and nudging options. The current study follows Bullock et al. [2014] by also nesting down to a 12-km domain covering the eastern U.S. over the area shown in Fig. 1 with a mesh of 292 by 223 grid cells in the x and y directions, respectively. Here, initial and lateral boundary conditions are provided by the inner nest from the 108- and 36-km domain configuration described in Otte et al [2012]. WRF version 3.4.1 [Skamarock et al., 2008] is used to simulate the two-year period 1 Nov. 2005 to 1 Dec. 2007. The initial 30 days of this period are taken as spin-up for the WRF model, and additional steps needed for the spin-up of the lake state in WRF-FLake are described in section 2e. The model top is set at 50 hPa, with 34 vertical half-sigma levels. The physics parameterizations chosen are the WRF Single-Moment 6-class microphysics scheme (WSM6) [Hong and Lim, 2006], Grell 3D ensemble cumulus parameterization [Grell and Dévényi, 2002], the Yonsei University (YSU) [Hong et al., 2006] planetary boundary layer (PBL) scheme, the Noah land surface model [Chen and Dudhia, 2001], and the Rapid Radiative Transfer Model for Global Climate Models (RRTMG) schemes for both longwave and shortwave radiation [Iacono et al., 2008]. Spectral nudging [Miguez-Macho et al., 2004] of potential temperature, horizontal wind components, and geopotential height is used to constrain the synoptic scale to the driving fields while allowing finer-scale features of the simulation to evolve. In the present study, spectral nudging toward R2 is applied on the 12-km domain at wavenumber 2 and below, resulting in nudging at wavelengths above 1800 and 1330 km in the x- and y-directions, respectively. These scales exceed those resolved by the R2 (using the $4\Delta x$ criterion [Grasso, 2000]). Nudging coefficients of $1 \times 10^{-4}\ s^{-1}$ for each field are used, and no nudging is applied below the PBL.

b.) Options for setting LSTs and ice coverage in WRF

The WRF Preprocessing System (WPS) has multiple options for interpolating various fields in the input dataset onto the WRF grid. When assigning the skin temperature over inland water points, the default interpolation options dictate that if no nearby water points are available in the input dataset for bilinear or weighted average interpolation, the closest water point is used (referred to in the documentation as the "search" option). This circumstance can occur when inland water bodies present in the fine resolution RCM are land points in the driving dataset because the input data are substantially coarser than the WRF grid, as is often the case for regional climate modeling and downscaling applications. The search method results in unrealistically sharp gradients between points, as neither linear interpolation nor any other averaging is done.

Figure 1 shows the land masks from R2 and the 12-km WRF domain. For R2, only three water points are present in the approximate area of Lakes Superior and Michigan, and the remaining Great Lakes (Huron, Erie and Ontario) are unresolved. In the 12-km WRF land mask, several interior lakes can be seen with no corresponding R2 points. The resulting interpolation of SST and ice coverage to 12-km grid spacing is also shown in Fig. 1. Water temperatures in Lakes Superior, Michigan, Huron, and most of Lake Erie are set from the three points present in the R2 dataset. However, at the eastern end of Lake Erie, the temperature abruptly changes, warming by nearly 20 K between adjacent grid points. This occurs because there are no surrounding R2 water points and the nearest R2 water point is in the Atlantic Ocean, resulting in oceanic SSTs being used to set water temperatures in eastern Lake Erie and throughout Lake Ontario. The use of this interpolation method also impacts smaller lakes within the domain, especially in the Southeast U.S. and Plains, where LSTs are set from warmer points in the Gulf of Mexico, hundreds of kilometers to the south.

Gao et al. [2012] addressed similar discontinuities in skin temperature by modifying the GCM land mask in the Great Lakes area, so that temperatures from land points in the GCM were used to set LSTs on the WRF grid. This treatment eliminates the need for the search algorithm and the abrupt LST gradients it produces. However, by using simulated land points from the GCM as water temperatures, effects of the contrasting lake and land temperatures are lost and the climate change feedbacks discussed in previous studies (e.g., Austin and Colman [2007], Kunkel et al., 2009, Gula and Peltier [2012]) cannot be simulated. Bullock et al. [2014] also reported unrealistic surface temperature gradients in the Great Lakes basin using the same domain configuration as in the present study to downscale R2. They employed the alternative lake treatment available in WRF version 3.3, setting LSTs using 2-m temperatures averaged from the previous month. Because 2-m air temperatures in the Great Lakes region are frequently below freezing during the winter months, this alternative lakes method resulted in unrealistically cold LSTs and widespread, persistent ice coverage.

Figure 1 also shows a snapshot of wintertime ice fraction using interpolation from R2, with abrupt and unrealistically large spatial coverage of ice resulting across Lakes Superior and Michigan. Large sections of those lakes are represented by only a single point on the R2 grid. As will be shown later, the remaining lakes have no ice cover because there are no R2 water points close enough to interpolate ice values from. This represents somewhat of a change from how temperatures at inland water points are prescribed because the default interpolation options for sea ice in WPS do not include the search method. Instead 0% ice coverage is prescribed when no neighboring points are available in the coarser dataset from which to interpolate ice concentrations.

While using ~1.9^{o} SST data from R2 for a 12-km run is unconventional for a historical simulation (because higher-resolution observed SSTs are available), using higher-resolution data in these retrospective runs would be counterproductive to the goal of our experiment: choosing a methodology to downscale GCM projections. When applying our methodology to future GCM projections, we will be constrained to use information at the resolution of the global model. If we chose to prescribe high-resolution observed LST analyses or climatologically-derived LSTs in a future climate, this would introduce an unrealistic stabilizing effect by imposing cooler present-day surface temperatures in a future warmer environment. Additionally the use of climatological LSTs would not account for interannual variability of lake temperatures and ice. Observational studies such as Austin and Colman [2007] and Burnett et al. [2003] highlight the importance of feedbacks between lake temperatures, ice and changes in the overlying atmosphere, while the modeling studies of Wright et al. [2013] and Notaro et al. [2013] cite the need for accurate prediction of LSTs and ice by lake models when simulating future climate states.

c.) FLake model

Gula and Peltier [2012] described regional downscaling WRF runs with LSTs and ice coverage simulated by an offline version of the FLake model that was driven using output from a GCM. When downscaling a GCM for a 30-year historical period, the inclusion of FLake-simulated lake temperatures and ice coverage improved the representation of rain and snowfall in the lee of the Great Lakes, relative to using LSTs taken from the GCM. The present work utilizes a version of WRF dynamically coupled to FLake.

FLake is a 1D column model, consisting of a two-layer parametric representation of a time-varying temperature profile [Mironov, 2008]. The top layer consists of a homogenous mixed layer (ML) and a stratified thermocline extending downward from the bottom of the ML. The second layer is representative of a layer of thermally-active sediment. Self-similarity theory, which originates from observed ocean ML dynamics [Kitaigorodskii and Miropolsky, 1970], is used to assign a shape to the thermocline, as well as the temperature profile within the bottom sediment layer. An integral energy budget is used for each of the two layers. Convective entrainment, wind-driven mixing, and solar heating of the water column are all considered to compute ML depth. FLake also has a separate parameterization for simulating lake ice and snow accumulating on top of the ice; however, snow accumulation on lake ice is not represented in the current version of the coupled WRF-FLake.

The atmospheric variables which must be supplied to FLake from a model or analyzed dataset are: 10-m windspeed, 2-m temperature and specific humidity, and downwelling shortwave and longwave radiation at the surface. Within the dynamical coupling framework of WRF-FLake, these variables are passed to FLake at every WRF time step and the surface temperature and lake ice at each lake point are passed back to WRF. Here, FLake is used with lake depths prescribed from the Global Lake Dataset [Kourzeneva, 2009]. Following FLake's documentation, as well as other studies [e.g., Mironov, 2008; Martynov et al., 2010], lake depth is capped at 60 m and the layer of thermally-active sediment is disabled at points where actual lake depth exceeds this cap. This "virtual bottom solution" is suggested because FLake's two-layer parametric representation (which assumes that the thermocline extends from the ML to the lake bottom) limits its ability to represent large, deep lakes. FLake accounts for processes, such as convective and mechanical mixing, which are most active in the upper layer of the lake (epilimnion), but FLake does not account for the presence of the hypolimnion (bottom layer of dense water between the thermocline and the lake bottom) which is present in large, deep lakes [Perroud, 2009; Balsamo, 2012].

FLake is a well-tested model, having been coupled with several different RCMs [e.g., Kourzeneva et al., 2008; Martynov et al., 2008; Mironov et al., 2010; Samuelsson et al., 2010)] and evaluated against other comparable lake models [e.g., Martynov et al., 2010; Pour et al., 2012; Semmler et al., 2012]. Martynov et al. [2010] conducted a sensitivity study of lake ice and temperatures using FLake and another 1D lake model. They found that both models perform best for smaller, shallower lakes and that FLake generally outperformed the other 1D model in the Great Lakes. However, both lake models failed to capture the typical pattern of springtime warming in the deep Great Lakes, suggesting that the absence of 2D and 3D processes (such as lake currents, ice drift, and the formation of a thermal bar) negatively affect FLake's performance as they would any other column model. Despite this limitation, Martynov et al. [2010] found that FLake adequately reproduced LSTs and ice coverage, as was also found by Gula and Peltier [2012], Semmler et al. [2012] and Pour et al. [2012].

Coupling the FLake model with WRF is advantageous because it is a column model reliant on empirical relationships, requiring relatively few atmospheric variables and prescribed lake depths. It is computationally efficient, requires little information about future lake characteristics, and its implementation within the source code can be easily modified with future WRF updates. A more sophisticated lake model may not have these qualities, and the added computational burden could hamper the ability to use the coupled lake model at finer resolutions for climate simulations.

d.) Observations

Observed LSTs are taken from the Advanced Very High Resolution Radiometer (AVHRR) dataset produced by the Group for High-Resolution SST (GHRSST) at the National Climatic Data Center [Reynolds et al., 2007]. This is a 0.25° product derived from satellite data that are bias corrected with ship and buoy observations. Simulated LSTs at points where lake ice is present are also validated against a Moderate Resolution Imaging Spectroradiometer (MODIS) land surface temperature dataset. This MODIS product (MOD11C2) is available in 8-day composites at 0.05° (~5.6 km) grid spacing. MODIS land surface temperatures have been shown to have an accuracy of better than 1 K over a temperature range of 263 to 300 K when validated over lake sites [Wan et al., 2002]. Fractional ice coverage data are taken from the National Ice Center's (NIC) Great Lakes Ice Analysis charts, which are based on observations from an ensemble of satellites, including the AVHRR, MODIS, and Geostationary Operational and Environmental Satellite (GOES) [Wang et al., 2012]. The NIC ice analysis is available twice weekly at a resolution of 2.5 km during the period simulated here.

For the purposes of evaluating the effect that different lake representations have on WRF's simulation of surface variables, hourly observations of 2-m temperature from the NOAA Meteorological Assimilation Data Ingest System (MADIS) were used for 2006 and 2007. Over 11,000,000 hourly observations are available in the MADIS dataset within the model domain during 2006 alone [Bullock et al., 2014]. The Atmospheric Model Evaluation Tool (AMET) is used to pair point observations with the nearest model grid point and generate various statistical products for near-surface fields [Appel et al., 2011]. The University of Delaware's global rainfall dataset is used for evaluating simulated precipitation. This 0.5° dataset (version 3.01) contains monthly mean precipitation values from 1901 to 2010. For the purposes of evaluation, the dataset was interpolated to the 12-km model domain.

e.) Simulations

In this study, three WRF simulations are conducted to examine how choices made in the downscaling configuration impact the setting of lake variables and the resulting simulation of important surface variables. The first, "CTLR2," uses WRF's default method for setting LSTs and lake ice by interpolation from R2. The result of such interpolation methods are discussed above and shown in Fig. 1.

The "WRF-FLake" simulation uses the same initial and boundary conditions (including oceanic SSTs and sea ice) as in CTLR2, but with lake ice concentrations and LSTs simulated by the dynamically-coupled FLake model. In order to provide the needed spin-up time for the lake model in a computationally efficient manner, the offline version of the FLake model was driven by R2 in a 10-cycle perpetual-year simulation, where the atmospheric conditions from 2005 were repeated until the lake model achieved equilibrium [Mironov et al., 2010]. The resulting LSTs (valid at 1 Nov 2005) were used to initialize WRF-FLake.

The third downscaled run examined in this study, "CTLOb," uses the NIC ice concentrations and GHRSST only over lake points. In the CTLOb simulation, R2's SST and sea ice fields are still utilized over ocean points in order to maintain consistency with the CTLR2 and WRF-FLake runs. The CTLOb run is a "best case scenario," where available products that are closer to the scale of the 12-km grid are utilized. CTLOb serves as a benchmark for the performance of the WRF model when LSTs and ice are prescribed from historical analyses that resolve the lakes well. However, it should be recognized that this option is not available for future climate simulations.

3. Results

a.) Lake surface temperatures

Figure 2 shows daily-averaged LSTs within the Great Lakes, taken collectively and separately, from all three simulations. The CTLR2 run is consistently too cool throughout the year for four of the five lakes, when compared with the benchmark CTLOb simulation. Warmer LSTs are prescribed in Lake Ontario, where LSTs are set using an Atlantic SST. WRF-FLake exhibits a somewhat exaggerated annual cycle, with LSTs too warm in the boreal summer. Across Lakes Superior, Michigan and Huron, FLake-simulated LSTs begin to warm rapidly approximately 1 month earlier than in CTLOb and the resulting overestimated LSTs persist into the summer months. The tendency of FLake to warm too early in the spring for large, deep lakes has been noted by prior RCM studies [Martynov et al., 2010; Samuelsson et al., 2010]. Overestimation of LSTs by FLake is reduced as the simulation progresses to the fall and winter periods.

Reynolds et al. [2007] describe the algorithm employed in the GHRSST dataset to produce a simulated SST at ice-covered points with a prescribed minimum value set at freezing. In the CTLOb run, subfreezing water temperatures can occur because WRF adjusts water temperatures to be consistent with the presence of ice prescribed from the NIC dataset. When WRF's fractional ice setting is used, the model overwrites some water temperature values as a function of ice cover. The purpose of this capability is to reconcile ice and SST data which may be inconsistent because they come from independent datasets (Keith Hines [Byrd Polar Research Center] and wrfhelp@ucar.edu, personal communication, 2014). Therefore, MODIS surface temperatures are used to evaluate simulated LSTs where ice is present. MODIS surface temperature over lake sites have been validated at several degrees below freezing and found to have errors less than 1 K [Wan et al., 2002]. Previously, Pour et al. [2012] used MODIS lake temperatures to evaluate 1D lake models. However, MODIS suffers from missing data in cloudy areas. Therefore, we use GHRSST (without the previously-described temperature adjustments by WRF) for validation in non-freezing conditions, and the MODIS product is employed for evaluation of grid cells with ice cover.

Table 1 lists the simulation-average mean absolute error (MAE) relative to GHRSST in open water conditions (where ice cover is zero) and then relative to MODIS at points with non-zero ice cover. WRF-FLake performs best for Lake Erie, the shallowest and smallest lake of the five studied here, while its MAE is greatest for the deepest and largest lake, Superior. Relative to CTLR2, WRF-FLake features lower or equal MAE in four out of five lakes and the simulation-averaged MAE over all lakes is reduced by ~0.4 K in open-water conditions (Table 1). By contrast, the CTLR2 run performs poorly in Lake Erie (which is unresolved in R2; see Fig. 1), with large cool biases during the summer; while it is more accurate in Lake Superior, where R2 has at least a partial representation of the lake. In CTLR2, Lake Ontario's temperatures have relatively low MAE (equaling that of WRF-FLake), despite its water temperatures being set from the Atlantic. Overall, WRF-FLake's simulated temperatures show improvement over interpolated CTLR2 values.

Under ice conditions, WRF-FLake's simulation-average MAE over all five lakes is somewhat larger (~1 K) than for open-water cells. The highest MAE occurs across Lake Superior, with lower error across Lake Erie (Table 1). As noted previously, ice spatial coverage in CTLR2 is unrealistic (Fig. 1), with ice significantly under-represented in temporal averages (see section 3b). Therefore, we do not compare CTLR2's ice temperatures.

b.) Ice coverage

CTLOb, with fractional ice values prescribed from the NIC ice analysis, is used to evaluate the other two simulations' ice coverage. However, in making that comparison, it must be considered that the FLake model outputs ice thickness rather than fractional ice coverage. As a column model, FLake is not configured to simulate partial coverage of the cell. To account properly for fractional ice coverage, FLake would need to be modified to simulate two temperature profiles (representing the open and closed portions of the cell) and conserve the total heat content within the cell. In the current implementation of WRF-FLake, any grid point that FLake simulates with an ice thickness greater than zero is interpreted as having complete 100% ice cover.

We explored using the empirical relationships of Karvonen et al. (2012) between ice thickness and concentration for various ice categories based on the World Meteorological Association Egg code, but this would require keeping track of the ice's age, and it was decided this was outside the scope of the present study. Instead, in order to compare the fractional NIC values and WRF-FLake's effectively binary ice coverage, the NIC fractional ice concentrations are converted to binary using two different methods In one method, we apply a 50% threshold, where values greater or equal to that threshold are rounded up to 100% and values below 50% are rounded down to zero. Ice fields derived using this method are referred to as "NIC50" hereafter. As an upper bound on the spatial extent of ice, the fractional NIC values are also converted where non-zero values are rounded up to 100%. This "NIC0" approach is more consistent with FLake's treatment of ice, where even very thin ice thicknesses (which realistically should correspond to small fractional values) are expressed as full 100% coverage of the cell.

Observed ice is significantly increased between the 2006 and 2007 ice seasons, providing an opportunity to assess WRF-FLake's response and whether it can accurately simulate interannual variability. Overall, the model performs well at simulating ice cover in both years across each of the five Great Lakes (Fig. 3), with basin-wide coverage lying between NIC0 and NIC50 during both periods. Ice is somewhat over-predicted in Lake Superior, exceeding even the higher NIC0 averages in March and April of both years. WRF-FLake performs well in both Lakes Huron and Michigan, with simulated ice concentrations similar to NIC50 averages during both years. In Lake Ontario, simulated ice coverage generally lies between NIC0 and NIC50. WRF-FLake ice coverage is consistent with NIC50 averages in Erie during 2006 (the low ice period), while 2007 concentrations are under-predicted relative to NIC0. WRF-FLake significantly outperforms CTLR2 at simulating ice coverage; in CTLR2, ice is generally absent aside from three occurrences spanning six days in total, and occurring only in Lakes Superior and Michigan.

In order to compare the spatial extent of ice, average winter ice cover for both years is plotted in Fig. 4 for the WRF-FLake and CTLOb runs, with NIC values averaged in their original fractional form. CTLR2 average winter ice values (not shown) have the same spatial coverage as shown in Fig. 1 but with a maximum value of ~1%. WRF-FLake's ice coverage largely corresponds to the presence of ice in the NIC dataset used to drive CTLOb. The spatial extent of ice cover in Lakes Michigan and Ontario is especially well-simulated by WRF-FLake. In Lake Superior, ice cover in the interior and along the northern shore is over-predicted, and the extent of ice coverage in Lakes Erie and Huron is somewhat less than observed, especially during 2007. However, in each lake, the representation of ice in WRF-FLake is significantly improved over CTLR2, which prescribed essentially no ice cover across the Great Lakes in either year.

c.) 2-m temperature

Lakes are a source of turbulent heat fluxes (which are inhibited by ice cover) and have a profound impact on regional climate. Therefore, it can be expected that improvement in the representation of LSTs and ice by WRF-FLake will increase the accuracy of nearby temperatures inland as well. The MAE of 2-m temperature is evaluated by comparison to MADIS surface observations during 2006 for sites in the Great Lakes basin (Fig. 5). In CTLR2, some near-shore points have a noticeably higher MAE relative to nearby inland points (see northern Lakes Michigan and Huron and along Lake Erie's shore). Both the CTLOb and WRF-FLake runs show reduced error in near-shore points relative to CTLR2. A similar comparison holds for 2007 (not shown).

Spatially-averaged plots of 2-m temperature bias taken over the Great Lakes basin and over the whole domain are shown for each season in Fig. 6. A systematic cool bias is found which persists through each season (with the sole exception of the fall of 2006), and is present not only in the Great Lakes region but in the domain averages as well. Though all simulations have a cold bias, CTLR2 generally has the largest bias, most dramatically in spring and summer in the Great Lakes basin. The erroneously cool LSTs in CTLR2 (Fig. 2) are likely responsible for the underestimation of 2-m temperatures, especially at near-shore sites.

The Great Lakes regional bias and MAE are summarized in Table 2. Averaged over the two-year simulation, WRF-FLake improves biases by ~0.4 K relative to CTLR2. CTLOb has the lowest MAE of the three runs in the Great Lakes area, but WRF-FLake actually outperforms

CTLOb in terms of bias. Much of this improvement occurs during the spring and summer months when the model tends to warm LSTs too aggressively (Fig. 2). This suggests that the overestimated LSTs in WRF-FLake are counteracting WRF's tendency to underestimate 2-m temperatures in this region.

d.) Precipitation

Figure 7 shows monthly averaged precipitation over the Great Lakes basin from each of the simulations compared with observed monthly rainfall from the University of Delaware. All three runs consistently overproduce precipitation throughout the simulated period, with WRF-FLake having an even more pronounced wet bias than the other two runs. This result is consistent with the cooler LSTs prescribed in CTLR2. WRF-FLake's warmer LSTs provide further surface heating to drive increased evaporation, convection, and precipitation. The fact that the CTLOb run, which provides the best realization of LSTs and ice, nevertheless has a greater error in monthly mean rainfall than CTLR2 indicates a pervasive problem in the simulations being compared here. Bullock et al. [2014] downscaled the same GCM-proxy, R2, as used here with a similar model set-up and also found positive biases in monthly rainfall even when employing different nudging strategies and physics choices. A number of studies indicate that the atmosphere analyzed in the R2 dataset is too moist and produces too much rainfall. Amenu and Kumar [2005] conclude that water vapor in R2 is globally positively biased relative to the National Aeronautics and Space Administration (NASA) Water Vapor Project (NVAP) data. Other regional studies have found wetter values (with respect to precipitable water vapor or precipitation) in the R2 compared with observations and other analyses [Bock and Nuret, 2009; Lim et al., 2011]. Park et al. [2008] and Winter and Eltahir [2012] both found wet biases in precipitation when downscaling the R2 with the Regional Climate Model version 3 (RegCM3). We speculate that excessive water vapor in the R2 could be contributing to the wet bias found here, but the validation of water vapor in R2 is beyond the scope of this study.

Comparison with the University of Delaware rainfall data is dominated by the wet bias of the three runs, so further discussion will focus on the comparison of the runs to each other in context with prior studies. Wright et al. [2013] compared the intensity and spatial extent of precipitation in a control run driven by observed LSTs and ice with idealized runs with either no ice or total coverage and a third idealized run where LSTs were increased by 3 K uniformly. They found that the existence of ice tended to suppress lake-effect snow, while warmer LSTs increased the spatial extent and intensity of lake-effect precipitation. In this study, CTLR2 is unrealistically absent of ice (Fig. 3) but has cooler LSTs than observed (Fig. 2). The former condition would lead to more lake-effect precipitation in CTLR2 than in CTLOb, but the latter would suppress precipitation in CTLR2. As CTLR2 has a lower wet bias than CTLOb, the dominant effect is from the cooler LSTs here.

Figure 8 presents the seasonally-averaged differences (taken from both years) between WRF-FLake and CTLR2. As expected, differences tend to be largest over and in the lee of the lakes with more precipitation in WRF-FLake, where LSTs are increased relative to the control run (Fig. 2). Plots comparing CTLOb and CTLR2 (not shown) are similar, with enhanced precipitation in CTLOb where lake temperatures are warmer than in CTLR2. The largest differences in precipitation are in the summer months. During this “lake stable” season, lake temperatures are cooler than overlying air temperatures, suppressing convection in the Great

Lakes basin. In early fall, atmospheric temperatures cool while LSTs remain relatively warm, supplying latent and sensible heat fluxes to the atmosphere and promoting convection during the "lake unstable" season. During the winter, these fluxes are impeded as the lakes freeze over. The capability of FLake to parameterize turbulent fluxes, radiative heating of the water column and the presence of a convectively-driven ML enables it to simulate such interactions between the lake and the overlying airmass.

Figure 9 shows basin-averaged 2-m temperatures and LSTs for each run, with shading to indicate the climatological lake unstable season. During the summer, when the region is expected to be in the lake stabilizing season, the difference between LSTs and 2-m temperatures is greater in the CTLR2 run than in CTLOb or WRF-FLake. The erroneously cool LSTs in CTLR2 enhance the stability on the overlying atmosphere in the Great Lakes basin and suppress lake-effect precipitation. The early warm-up of spring LSTs in WRF-FLake lessens the difference between atmospheric and lake temperatures, reducing the imposed stability. During the fall months, the relative warmth of lake temperatures compared to air temperatures is more pronounced in WRF-FLake than in CTLR2, enhancing lake-effect precipitation in the former simulation during the early months of the lake unstable season. Overall, the cool bias in CTLR2 water temperatures enables this run to perform better in terms of basin-averaged monthly precipitation, despite having an inferior representation of the lake state in terms of LSTs and ice coverage.

4. Summary

The results of downscaling the R2 reanalysis as a representative GCM-proxy are investigated with regard to how lakes are treated when few inland water points are present in the coarser dataset to provide information to a regional WRF simulation. Two-year simulations are conducted, one using lake information interpolated from R2 (CTLR2), one using lake temperatures and ice set from higher-resolution analyses (CTLOb), and one in which a column lake model, FLake, is dynamically coupled with WRF (WRF-FLake). In CTLR2, only three water points are available to set water temperatures across the Great Lakes when downscaling to a 12-km grid (Fig. 1). Using the WPS's default interpolation options, this results in abrupt and unrealistic gradients in lake temperatures, as some lake grid cell temperatures are set using temperatures from the nearest water grid cell in the GCM-proxy, even if it represents an oceanic temperature (Fig. 1). Ice cover in CTLR2 is also found to be poorly prescribed, as deep lakes abruptly freeze almost completely.

The goals of this study are to assess the consequences of using a coarse dataset to set temperature and ice at inland water points and to examine whether using the FLake model can improve the simulation. Overall, it has been demonstrated that the representation of lake surface temperatures, 2-m temperatures and ice coverage have all been improved by the use of WRF-FLake. The most dramatic improvement in the representation of inland lakes by WRF-FLake over CTLR2 is in its simulation of lake ice. Ice coverage produced by CTLR2 occurs for only two of the Great Lakes over three short, non-contiguous periods during the entire two-year simulation (Fig. 3). When ice does appear, it covers almost the entirety of Lakes Superior and Michigan and then disappears completely within a 1-hour period (Fig. 1). Meanwhile, shallower lakes that often incur some winter freezing (like Erie), remain completely open through two winters because (in the coarser R2 dataset) no valid water points are close enough to set values of ice for the eastern-most Great Lakes. By contrast, WRF-FLake represents the spatial extent of ice well and is able to capture the increase in ice from the 2006 to 2007 winter seasons (Figs. 3 and 4).

Overall, LSTs are better represented in WRF-FLake than in CTLR2, even though the latter is an analyzed SST that has been prescribed rather than a simulated water temperature. In open water conditions, WRF-FLake LSTs have lower or equal MAE relative to CTLR2 in all but one of the five lakes compared (Table 1). The temperatures interpolated from CTLR2 are too cool throughout the year in each lake except Ontario, which has a prescribed water temperature set from the Atlantic (Figs. 1 and 2). Consistent with past work [Martynov et al., 2010; Samuelsson et al. 2010], this study finds that FLake performs best in shallower lakes, but it tends to warm too strongly in the spring across large, deep lakes (Fig. 2). Lake Erie is most improved by the use of the FLake model, while Lake Superior has the largest error in simulated LSTs.

Simulated 2-m temperatures in the Great Lakes basin are notably improved in WRF-FLake compared to CTLR2, with reductions in both MAE and mean bias (Table 2, Fig. 6). WRF-FLake reduces the averaged bias in 2-m temperatures in the Great Lakes basin by approximately 0.4 K. Conspicuously, the accuracy of simulated precipitation amounts is degraded by the use of the lake model, and precipitation is not well-simulated even when higher-resolution observational products are used to set lake variables, indicating systematic problems in either the WRF configuration used here or the R2 data being downscaled. Each of the three runs examined here produces too much precipitation, and the use of temperatures from the lake model increases WRF's wet bias (Fig. 7). CTLR2 has the lowest wet bias because of the compensating error in its LSTs, which are consistently cooler than observed. This imposed surface cooling increases the stability of the overlying air mass and reduces lake-effect precipitation.

This study serves to caution regional climate modelers to examine how inland water temperatures and ice are being set when using a similar methodology, as many currently-used downscaling procedures may not account for the undesired effects of using coarse datasets to set variables over inland water points. Previous studies (e.g., Gula and Peltier [2012], Notaro et al. [2013] and Wright et al. [2013]) highlight the need for accurate predictions of LST and ice cover. Past observational studies have shown non-linear effects of climate change in warming lake temperatures and decreasing ice cover, both of which enhance precipitation [Assel and Robertson, 1995; Burnett et al., 2003; Austin and Colman, 2007; Kunkel et al., 2009]. The use of a coupled lake model within an RCM, as done here, potentially enables the simulation of important feedbacks of climate change on regions affected by the presence of lakes.

Acknowledgements

The lead author was supported by an appointment to the Research Participation Program at the U.S. Environmental Protection Agency Office of Research and Development, administered by the Oak Ridge Institute for Science and Education (ORISE). The WRF model is made available by NCAR, funded by the National Science Foundation. We thank Drs. Jiming Jin and Lin Zhao of Utah State University for providing code for processing the NIC ice data. Thanks also to Dr. Kiran Alapaty for his contributions to the manuscript. The authors also appreciate the helpful comments of two anonymous reviewers on this article. The University of Delaware precipitation data was provided by the NOAA/OAR/ESRL PSD, Boulder, Colorado, USA, from their website at http://www.esrl.noaa.gov/psd/. This research has been subjected to the U.S. EPA's administrative review and approved for publication. The views expressed and the contents are solely the responsibility of the authors, and do not necessarily represent the official views of the U.S. EPA.

References

Amenu, G. and P. Kumar (2005), NVAP and Reanalysis-2 global precipitable water products: Intercomparison and variability studies. *Bull. Amer. Meteor. Soc.*, **86**, 245–256.

Appel, K. W., R. C. Gilliam, N. Davis, A. Zubrow, and S. C. Howard (2011), Overview of the atmospheric model evaluation tool (AMET) v1.1 for evaluating meteorological and air quality models. *Env. Modelling & Software*, **26**, 434-443.

Assel, R. A., and D. M. Robertson (1995), Changes in winter air temperatures near Lake Michigan, 1851–1993, as determined from regional lake-ice records. *Limnol. Oceanogr.*, **40,** 165–176.

Austin, J., and S. Colman (2007), Lake Superior summer water temperatures are increasing more rapidly than regional air temperatures, A positive ice–albedo feedback. *Geophys. Res. Lett.*, **34**, L06604, doi:10.1029/2006GL029021.

Balsamo, G., R. Salgado, E. Dutra, S. Boussetta, T. Stockdale, and M. Potes (2012), On the contribution of lakes in predicting near-surface temperature in a global weather forecasting model.*Tellus A*, **64**, 15829. doi:10.3402/tellusa.v64i0.15829

Bates, G. T., F. Giorgi, and S. W. Hostetler (1993), Toward the simulation of the effects of the Great Lakes on regional climate. *Mon. Wea. Rev.*, **123**, 1505-1522.

Bock, O. and M. Nuret (2009), Verification of NWP model analyses and radiosonde humidity data with GPS precipitable water vapor estimates during AMMA. *Wea. Forecasting*, **24**, 1085–1101.

Bullock, O. R., K. Alapaty, J. A. Herwehe, M. S. Mallard, T. L. Otte, R. C. Gilliam, and C. G. Nolte (2014), An observation-based investigation of nudging in WRF for downscaling surface climate information to 12-km grid spacing. *J. Appl. Meteor. Climatol.,* **53**, 20-33.

Burnett, A. W., M. E. Kirby, H. T. Mullins, W. P. Patterson (2003), Increasing Great Lake–effect snowfall during the twentieth century: A regional response to global warming? *J. Climate*, **16**, 3535–3542

Chen, F., and J. Dudhia (2001), Coupling and advanced land surface–hydrology model with the Penn State–NCAR MM5 modeling system. Part I: Model implementation and sensitivity. *Mon. Wea. Rev.*, **129**, 569–585.

Gao, Y., J. S. Fu, J. B. Drake, Y. Liu, J-F. Lamarque (2012), Projected changes of extreme weather events in the eastern United States based on a high resolution climate modeling system. *Environ. Res. Lett.*, **7,** doi:10.1088/1748-9326/7/4/044025.

Gerbush, M. R., D. A. R. Kristovich, N. F. Laird (2008), Mesoscale Boundary Layer and Heat Flux Variations over Pack Ice–Covered Lake Erie. *J. Appl. Meteor. Climatol.*, **47**, 668–682.

Grasso, L. D., 2000: The difference between grid spacing and resolution and their application to numerical modeling. *Bull. Amer. Meteor. Soc.*, **81,** 579–580.

Grell, G. A., and D. Dévényi (2002), A generalized approach to parameterizing convection combining ensemble and data assimilation techniques. *Geophys. Res. Lett.*, **29**, 1693, doi:10.1029/2002GL015311.

Gula, J., and W. R. Peltier (2012), Dynamical downscaling over the Great Lakes basin of North America using the WRF regional climate model: The impact of the Great Lakes system on regional greenhouse warming. *J. Climate*, **25**, 7723–7742.

Hong, S.-Y., Y. Noh, and J. Dudhia (2006), A new vertical diffusion package with an explicit treatment of entrainment processes. *Mon. Wea. Rev*., 134, 2318–2341.

Hong, S.-Y. and J. O. J. Lim (2006), The WRF single moment 6-class microphysics scheme (WSM6). *J. Korean Meteor. Soc*., 42, 129–151.

Iacono, M. J., J. S. Delamere, E. J. Mlawer, M. W. Shephard, S. A. Clough, and W. D. Collins (2008), Radiative forcing by long-lived greenhouse gases: Calculations with the AER radiative transfer models. *J. Geophys. Res.*, **113**, D13103, doi:10.1029/2008JD009944.

Kanamitsu, M., W. Ebisuzaki, J. Woollen, S.-K. Yang, J. J.Hnilo, M. Fiorino, and G. L. Potter (2002), NCEP–DOE AMIP-II Reanalysis (R-2). *Bull. Amer. Meteor. Soc.*, **83**,1631–1643.

Karvonen, J., Cheng, B., Vihma, T., Arkett, M., and Carrieres, T. (2012), A method for sea ice thickness and concentration analysis based on SAR data and a thermodynamic model, *The Cryosphere*, **6**, 1507-1526, doi:10.5194/tc-6-1507-2012, 2012.

Kitaigorodskii, S. and Y. Miropolsky (1970), On the theory of the open ocean active layer. *Izv. Atmos. Ocean. Phy.*, **6**, 178-188.

Kourzeneva, E., Samuelsson, P., Ganbat, G. and Mironov, D. (2008), Implementation of Lake Model FLake into HIRLAM. *HIRLAM Newsletter* 54, 54–64. Available from HIRLAM-A Programme, c/o J. Onvlee, KNMI, P.O. Box 201, 3730 AE De Bilt, The Netherlands. Online at: http://hirlam.org.

Kourzeneva, E. (2009), Global dataset for the parameterization of lakes in numerical weather prediction and climate modeling. *ALADIN Newsletter,*No. 37, ALADIN, Toulouse, France, 46-53.

Kunkel, K. E., L. Ensor, M. Palecki, D. Easterling, D. Robinson, K. G. Hubbard, and K. Redmond (2009), A new look at lake-effect snowfall trends in the Laurentian Great Lakes using a temporally homogeneous data set. *J. Great Lakes Res.*, **35**, 23–29.

Lim, Y., L. Sefanova, S. Chan, S. Schubert, J. O'Brien (2011), High-resolution subtropical precipitation derived from dynamical downscaling of the NCEP/DOE reanalysis: How much small-scale information is added by a regional model? *Clim. Dyn.*. **37**, 1061-1080.

Lofgren, B. M. (1997), Simulated effects of idealized Laurentian Great Lakes on regional and large-scale climate. *J. Climate*, **10**, 2847-2858.

Magnuson, J. J. and coauthors (2000), Historical trends in lake and river ice cover in the Northern Hemisphere, *Science*, **289**, 1743–1746.

Martynov, A., R. Laprise, and L. Sushama (2008), Off-line lake water and ice simulations: A step towards the interactive lake coupling with the Canadian Regional Climate Model. *Geophysical Research Abstracts*, **vol. 10**, EGU2008-A-02898, EGU General Assembly 2008.

Martynov, A., L. Sushama, and R. Laprise (2010), Simulation of temperate freezing lakes by one-dimensional lake models: Performance assessment for interactive coupling with regional climate models. *Boreal Environ. Res.*, **15**, 143–164.

Miguez-Macho, G., G. L. Stenchikov, and A. Robock (2004), Spectral nudging to eliminate the effects of domain position and geometry in regional climate model simulations. *J. Geophys. Res.*, **109**, D13104, doi:10.1029/2003JD004495.

Mironov, D. V. (2008), Parameterization of lakes in numerical weather prediction. Description of a lake model. *COSMO Technical Report*, No. 11, Deutscher Wetterdienst, Offenbach am

Main, Germany, 41 pp.

Mironov, D., E. Heise, E. Kourzeneva, B. Ritter, N. Schneider, and A. Terzhevik (2010), Implementation of the lake parameterisation scheme FLake into the numerical weather prediction model COSMO. *Boreal Env. Res.*, **15**, 218–230.

Notaro, M., K. Holman, A. Zarrin, E. Fluck, S. Vavrus, V. Bennington (2013), Influence of the Laurentian Great Lakes on regional climate. *J. Climate*, **26**, 789–804.

Otte, T. L., C. G. Nolte, M. J. Otte, J. H. Bowden (2012), Does nudging squelch the extremes in regional climate modeling? *J. Climate*, **25**, 7046–7066.

Park, E.-H., S.-Y. Hong, and H.-S. Kang (2008), Characteristics of an East–Asian summer monsoon climatology simulated by the RegCM3. *Meteorology and Atmospheric Physics*. doi:10.1007/s00703-008-0300-0

Perroud, M., S. Goyette, A. Martynov, M. Beniston, and O. Anneville (2009), Simulation of multiannual thermal profiles in deep Lake Geneva: A comparison of one-dimensional lake models. *Limnol. Oceanogr.*, **54**, 1574–1594.

Pour, H. K., C. R. Duguay, A. Martynov, and L. C. Brown (2012), Simulation of surface temperature and ice cover of large northern lakes with 1-D models: A comparison with MODIS satellite data and in situ measurements. *Tellus*, **64**, doi:10.3402/tellusa.v64i0.17614

Reynolds, R. W., T. M. Smith, C. Liu, D. B. Chelton, K. S. Casey and M. G. Schlax (2007), Daily high-resolution blended analyses for sea surface temperature. *J. Climate*, **20**, 5473-5496.

Samuelsson, P., E. Kourzeneva, and D. Mironov (2010), The impact of lakes on the European climate as simulated by a regional climate model. *Boreal Env. Res.*, **15**, 113-129.

Semmler, T., B. Cheng, Y. Yang, and L. Rontu (2012), Snow and ice on Bear Lake (Alaska) – sensitivity experiments with two lake ice models. *Tellus A*, **64**, 17339. doi:10.3402/tellusa.v64i0.17339

Sillmann, J., V. V. Kharin, X. Zhang, F. W. Zwiers and D. Bronaugh (2013), Climate extreme indices in the CMIP5 multi-model ensemble. Part 1: Model evaluation in the present climate, *J. Geophys. Res*., 118, doi: 10.1002/jgrd.50203.

Skamarock, W. C., J. B. Klemp, J. Dudhia, D. O. Gill, D. M. Barker, M. Duda, X.-Y. Huang, W. Wang and J. G. Powers (2008), A description of the Advanced Research WRF version 3. Tech. Rep. NCAR/TN-475+STR, 113 pp.

Wan, Z. M., Y. L Zhang, Q. C. Zhang, Z. L. Li (2002), Validation of the land-surface temperature products retrieved from Terra Moderate Resolution Imaging Spectroradiometer data. *Remote Sensing Of Environment*, **83**, 163-180.

Wang, J., R.A. Assel, S. Walterscheid, A. Clites, and X. Bai (2012), Great Lakes ice climatology update: Winter 2006–2011 description of the digital ice cover data set. NOAA Technical Memorandum GLERL-155, 37 pp.

Wilson, J. W. (1977), Effect of Lake Ontario on precipitation. *Mon. Wea. Rev.*, **105**, 207–214.

Winter, J.M., and E.A.B. Eltahir (2012), Modeling the hydroclimatology of the midwestern United States. Part 1: Current climate. *Clim. Dyn.*, **38**, 573-593, doi:10.1007/s00382-011-1182-2.

Wright, D. M., D. J. Posselt, A. L. Steiner, 2013: Sensitivity of lake-effect snowfall to lake ice cover and temperature in the Great Lakes region. *Mon. Wea. Rev.*, **141**, 670–689.

Zhao, L., J. Jin, S.-Y. Wang, M. B. Ek (2012), Integration of remote-sensing data with WRF to improve lake-effect precipitation simulations over the Great Lakes region. *J. Geophys. Res.*, **117**, doi:10.1029/2011JD016979.

Zulauf, M. A., and S. K. Krueger (2003), Two-dimensional cloud-resolving modeling of the atmospheric effects of Arctic leads based upon midwinter conditions at the Surface Heat Budget of the Arctic Ocean ice camp. *J. Geophys. Res.*, **108**, 4312, doi: 10.1029/2002JD002643

List of Tables

List of Figures

FIG. 5. 2-m temperature MAE (K), computed hourly against MADIS observations in the Great Lakes basin, averaged over the year 2006, and shown every 0.25 K from 0.75 to 3 K and every 1 K between 3 and 4 K.

FIG. 6. Seasonally-averaged bias (K), spatially averaged in the Great Lakes basin (top) and the eastern U.S. domain pictured in Fig. 1 (bottom), shown for each of the runs as denoted in the legend.

FIG. 7. Monthly average precipitation (shown in mm day^{-1}) taken over the Great Lakes basin for each of the model runs and plotted with monthly rainfall from the University of Delaware interpolated to the WRF domain.

FIG. 8. Differences (mm day^{-1}) in seasonally-averaged precipitation (averaged over both years) between WRF-FLake and CTLR2, where warm (cool) colors indicate more precipitation in the WRF-FLake (CTLR2) run.

FIG. 9. Daily LSTs (dashed) and 2-m temperature (solid) averaged over the Great Lakes basin for CTLOb (top), CTLR2 (middle) and WRF-FLake (bottom). The air temperatures have a 10-point smoother applied to filter out short term variability. Gray shading denotes the climatological lake unstable season. Note that the use of smoothing, as well as temporal and spatial averaging, de-emphasizes differences between the air temperatures simulated by the three runs.

TABLE 1. Mean absolute error (K) in daily LSTs in open water and ice conditions, averaged across each lake and over all five Great Lakes. Error relative to ice points in CTLR2 is not shown because only three days in the two-year simulation feature any ice for the first two lakes listed, while the remaining three lakes have no ice at any point in CTLR2.

	Open water points		**Ice points**
	CTLR2	WRF-FLake	WRF-FLake
All Great Lakes	2.95	2.56	4.35
Lake Superior	2.57	3.00	4.85
Lake Michigan	3.25	2.46	3.60
Lake Huron	2.67	2.43	4.12
Lake Erie	4.40	1.86	3.30
Lake Ontario	2.30	2.30	3.6

TABLE 2. Mean bias and MAE in 2-m temperature (K) from each of the simulations, taken over the Great Lakes basin and averaged over the 2-year simulation.

Run	Bias	MAE
CTLOb	-0.88	2.19
CTLR2	-1.12	2.29
WRF-FLake	-0.76	2.23

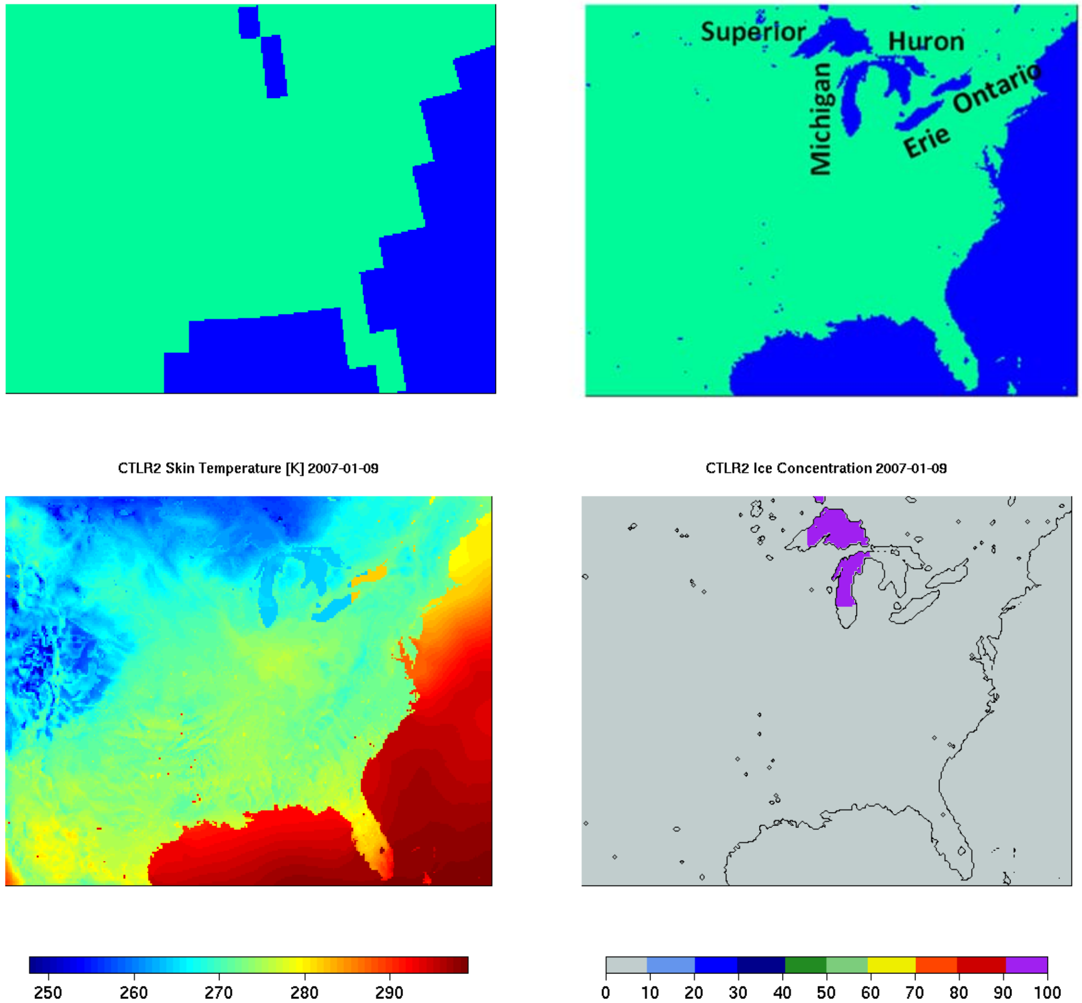

FIG. 1. The land mask used in the R2 data, as shown in the area corresponding to the 12-km eastern U.S. domain (top left) and the 12-km WRF grid's land mask (top right, shown with the lakes labeled). The skin temperature (K, bottom left) and ice cover (bottom right) interpolated from R2 to the 12-km grid, valid at 12 UTC 9 Jan 2007.

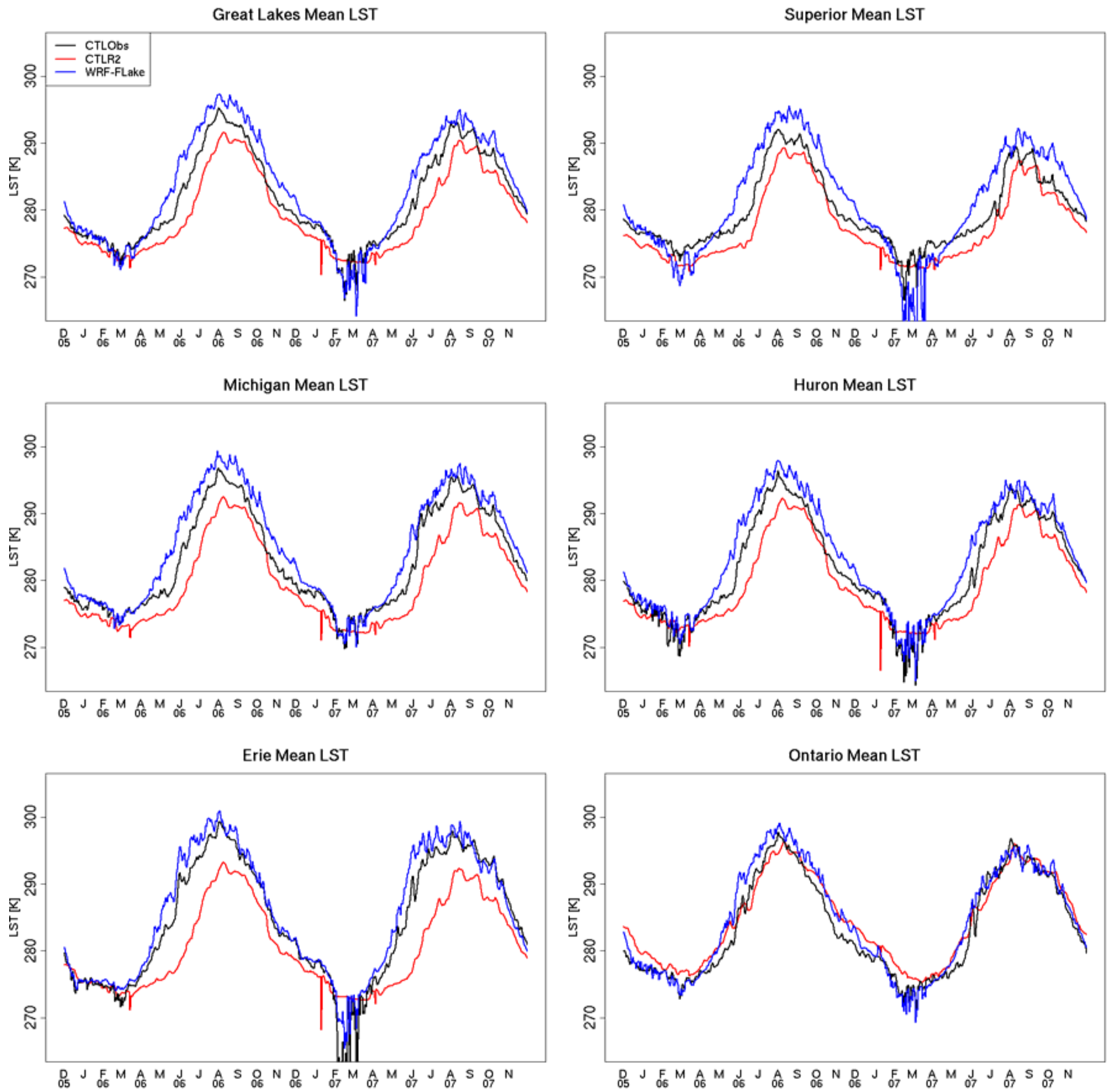

FIG. 2. Daily- and lake-averaged LSTs for all Great Lakes collectively (top left) and for Lakes Superior (top right), Michigan (middle left), Huron (middle right), Erie (bottom left) and Ontario (bottom right) with the CTLOb run shown in black, CLTR2 in red and WRF-FLake in blue.

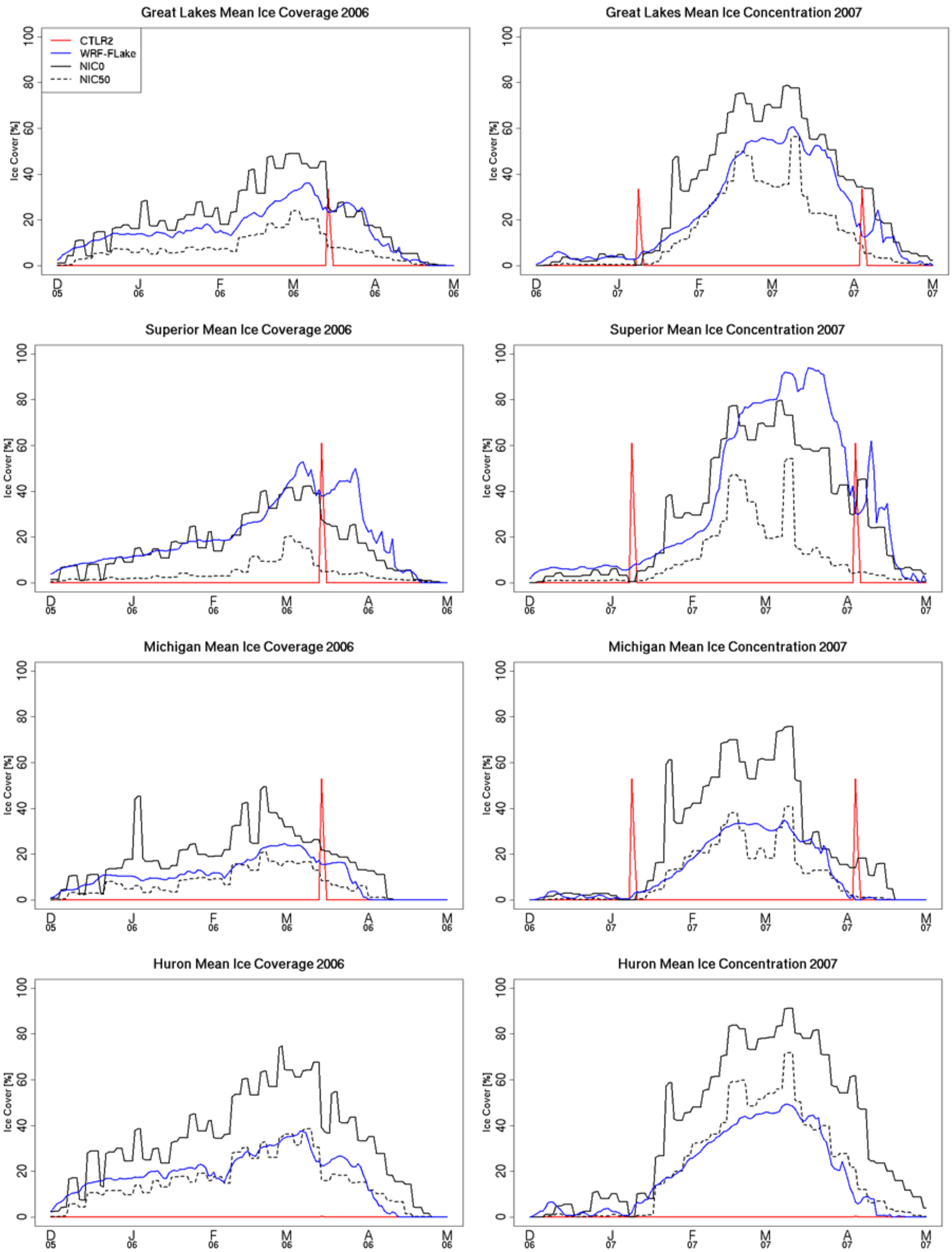
Great Lakes Mean Ice Coverage 2006
Great Lakes Mean Ice Concentration 2007
Superior Mean Ice Coverage 2006
Superior Mean Ice Concentration 2007
Michigan Mean Ice Coverage 2006
Michigan Mean Ice Concentration 2007
Huron Mean Ice Coverage 2006
Huron Mean Ice Concentration 2007
CTLR2
WRF-FLake
NIC0
NIC50
Ice Cover [%]
0
20
40
60
80
100
D 05
J 06
F 06
M 06
A 06
M 06
D 06
J 07
F 07
M 07
A 07
M 07

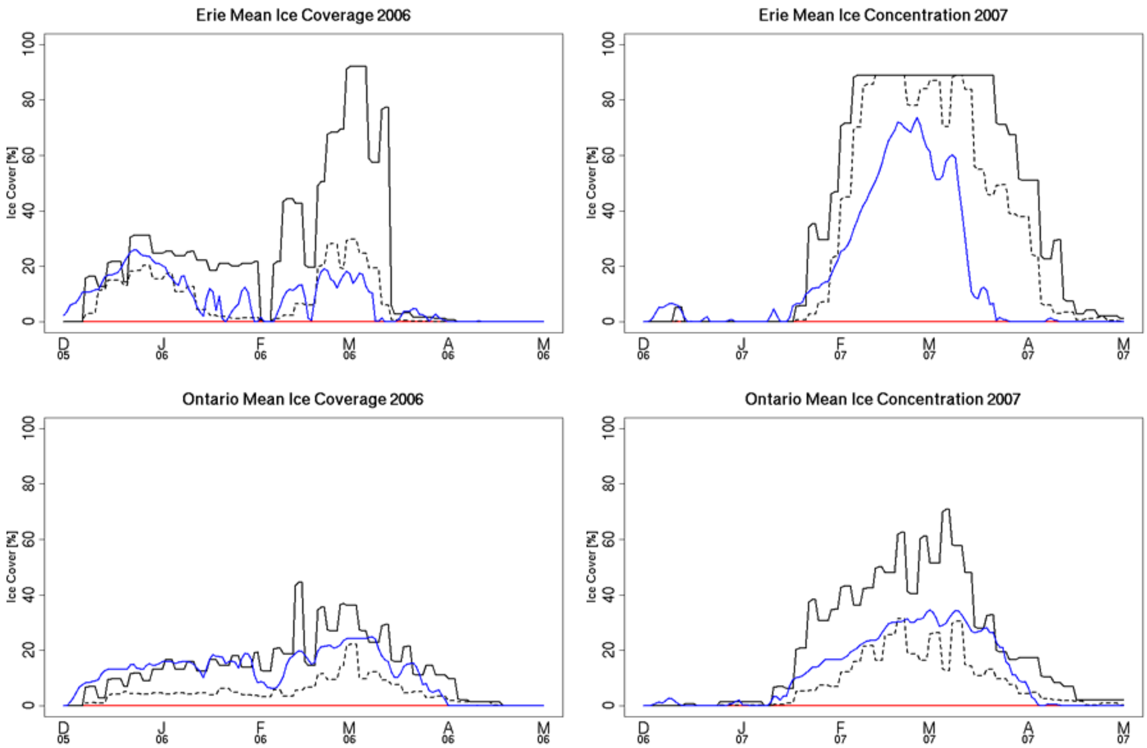

FIG. 3. Daily- and lake-averaged ice concentrations for all Great Lakes together and each individually are shown in the same order as in the previous figure, for the winter of 2005-2006 (left) and 2006-2007 (right). The solid and dotted black lines represent NIC0 and NIC50, respectively. Blue and red lines represent WRF-FLake and CTLR2 ice concentrations, respectively.

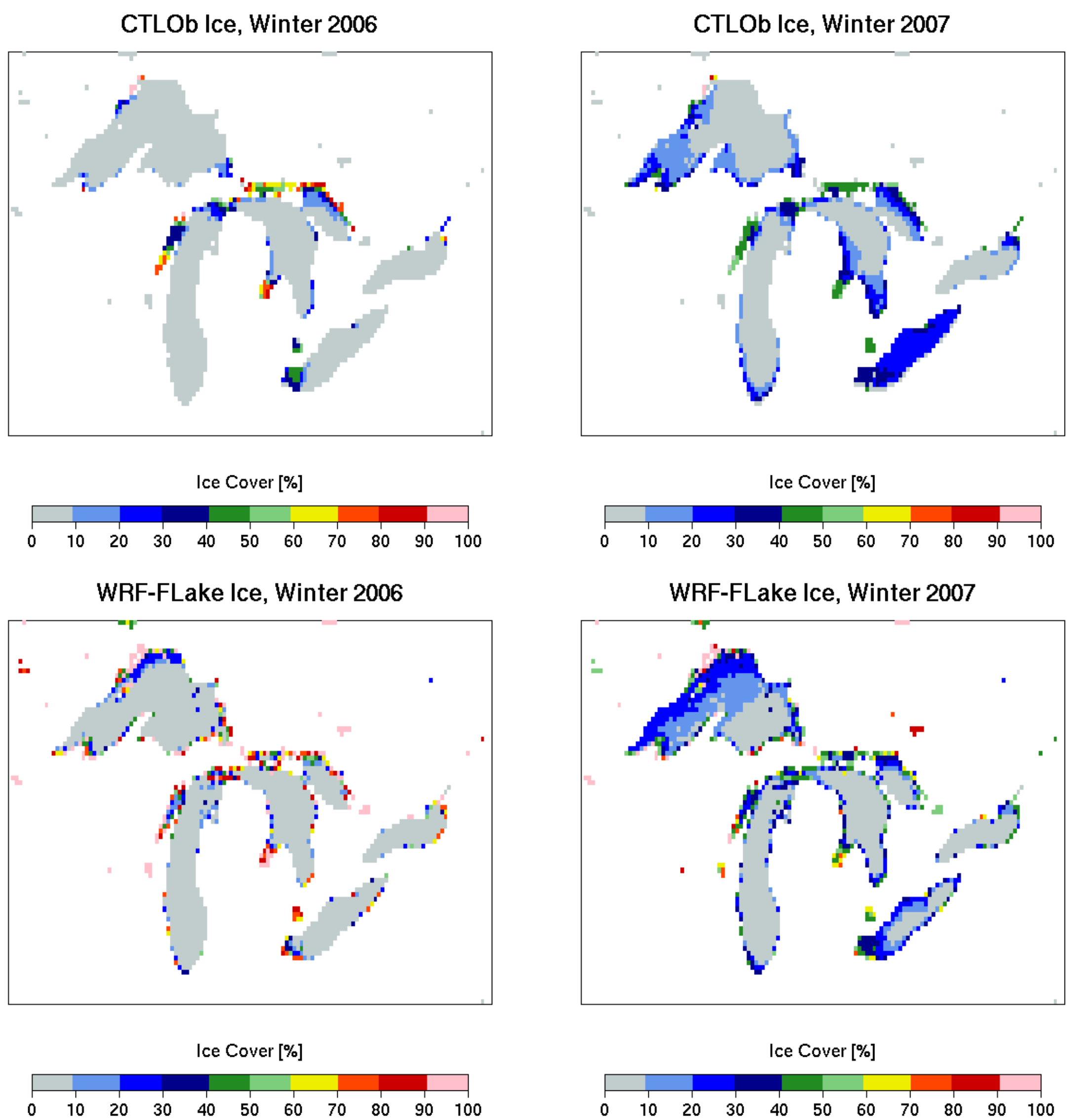

FIG. 4. Averaged winter (December through February) ice coverage from 2006 (left) and 2007 (right) from the CTLOb (top) and WRF-FLake (bottom) simulations. Here, the averages have been computed with the NIC values kept as a fractional dataset, so the imposed thresholds used to derive NIC0 and NIC50 are not applied.

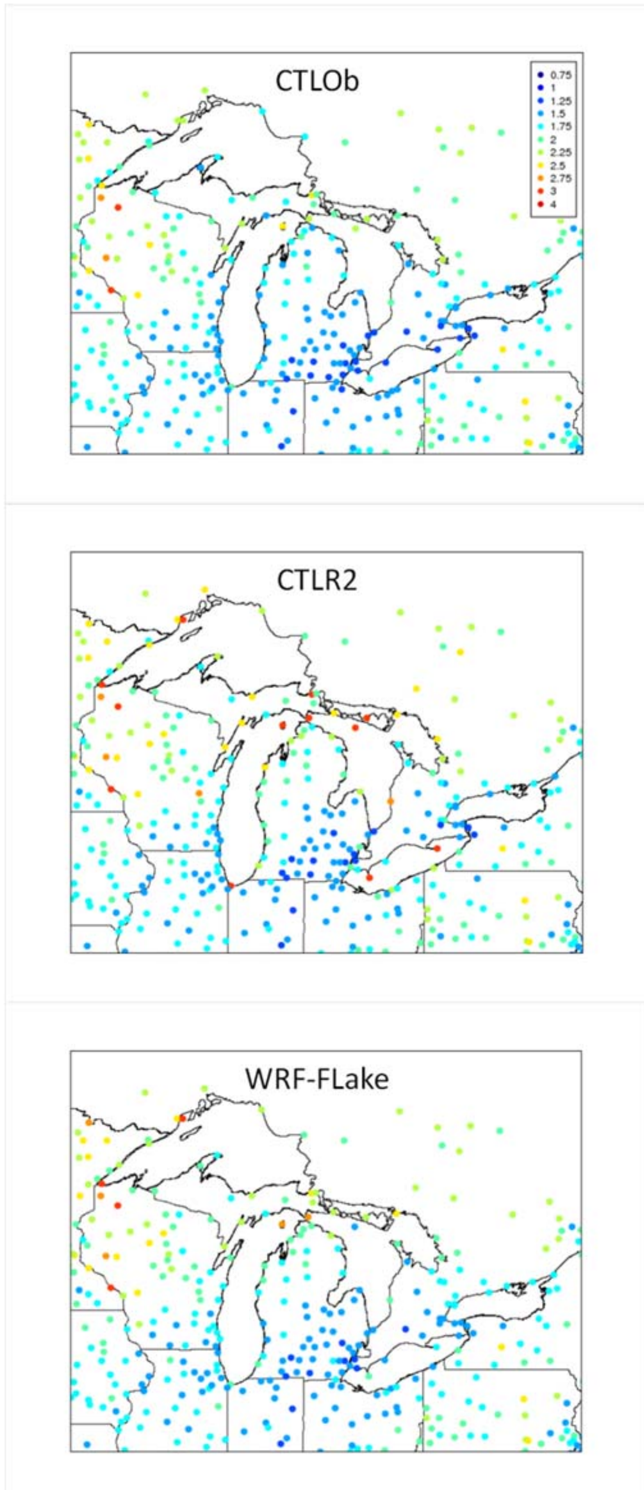

FIG. 5. 2-m temperature MAE (K), computed hourly against MADIS observations in the Great Lakes basin, averaged over the year 2006, and shown every 0.25 K from 0.75 to 3 K and every 1 K between 3 and 4 K.

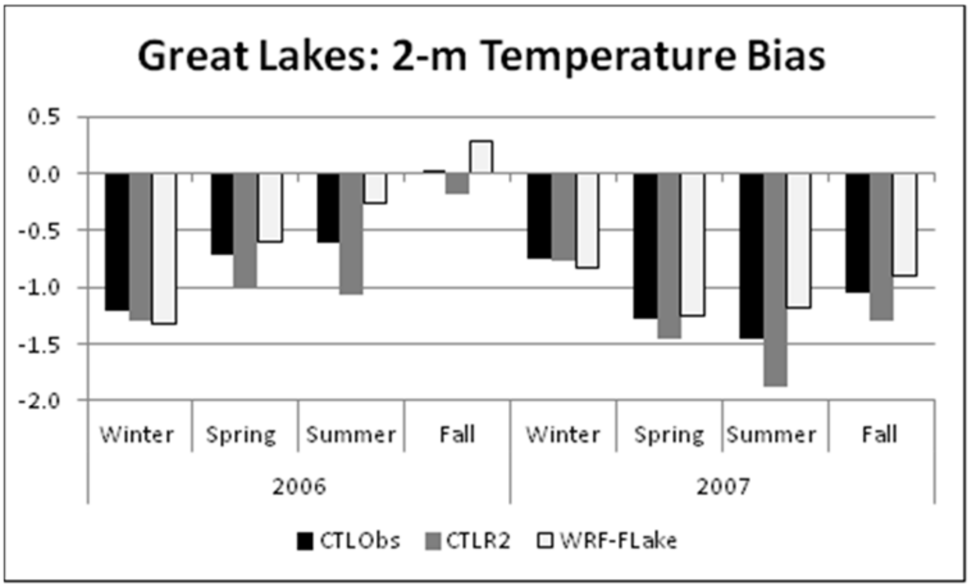

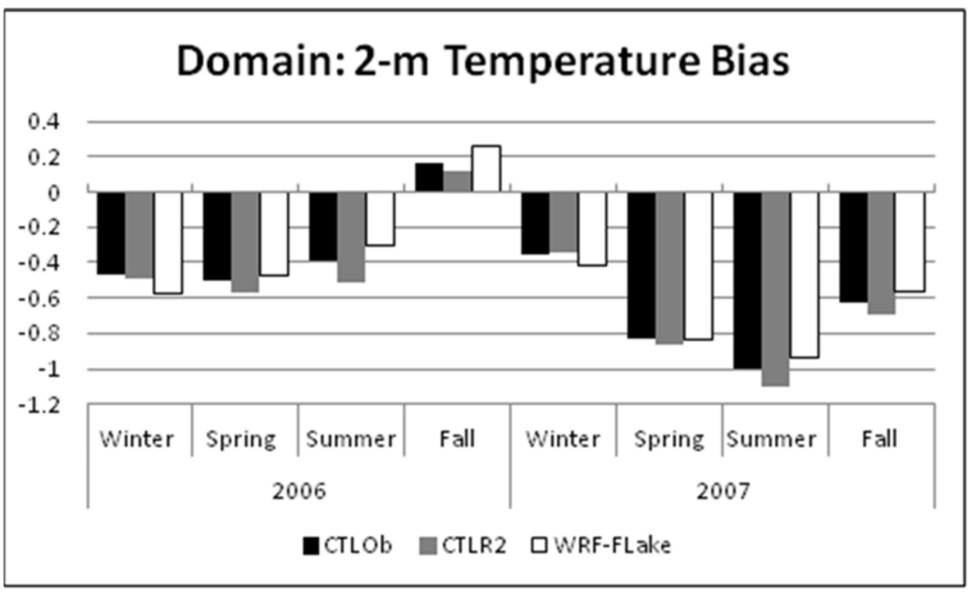

FIG. 6. Seasonally-averaged bias (K), spatially averaged in the Great Lakes basin (top) and the eastern U.S. domain pictured in Fig. 1 (bottom), shown for each of the runs as denoted in the legend.

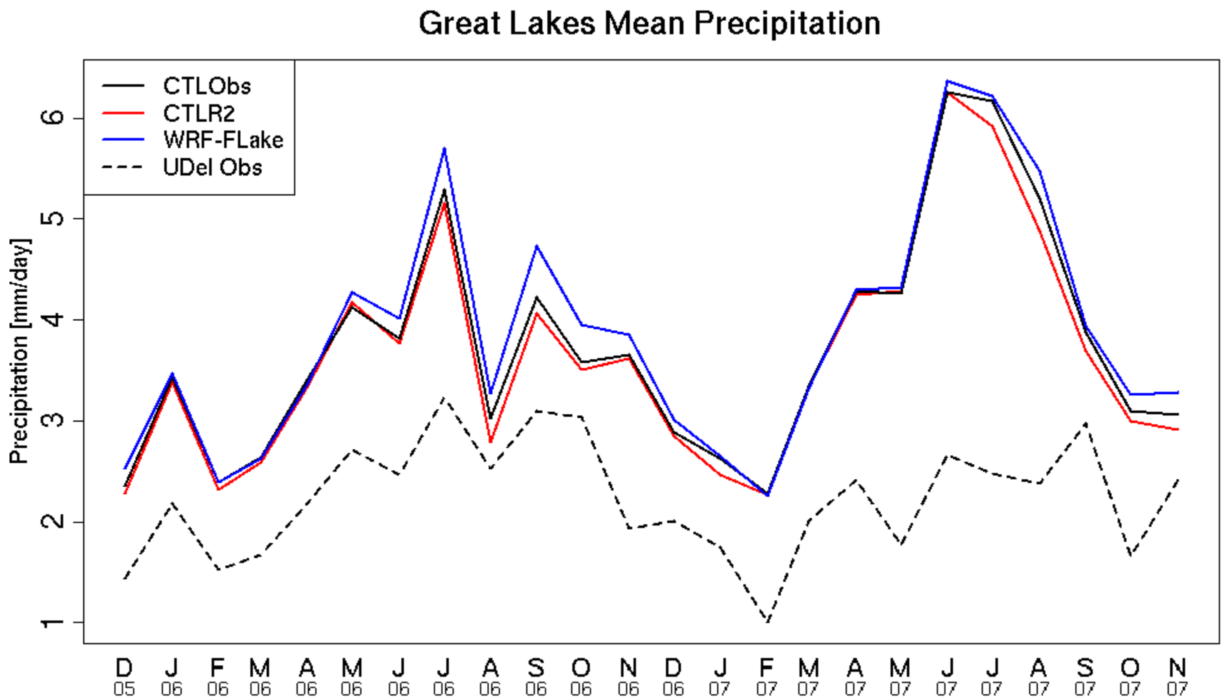

FIG. 7. Monthly average precipitation (shown in mm day^{-1}) taken over the Great Lakes basin for each of the model runs and plotted with monthly rainfall from the University of Delaware interpolated to the WRF domain.

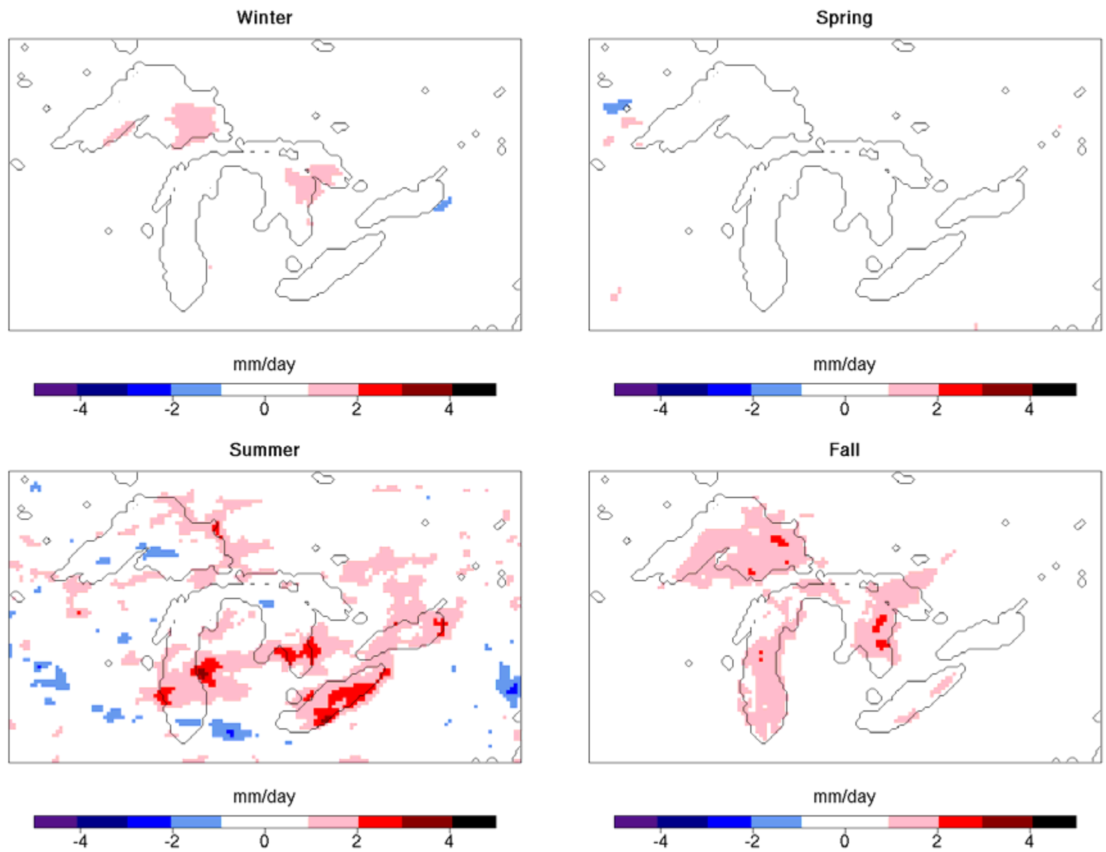

FIG. 8. Differences (mm day^{-1}) in seasonally-averaged precipitation (averaged over both years) between WRF-FLake and CTLR2, where warm (cool) colors indicate more precipitation in the WRF-FLake (CTLR2) run.

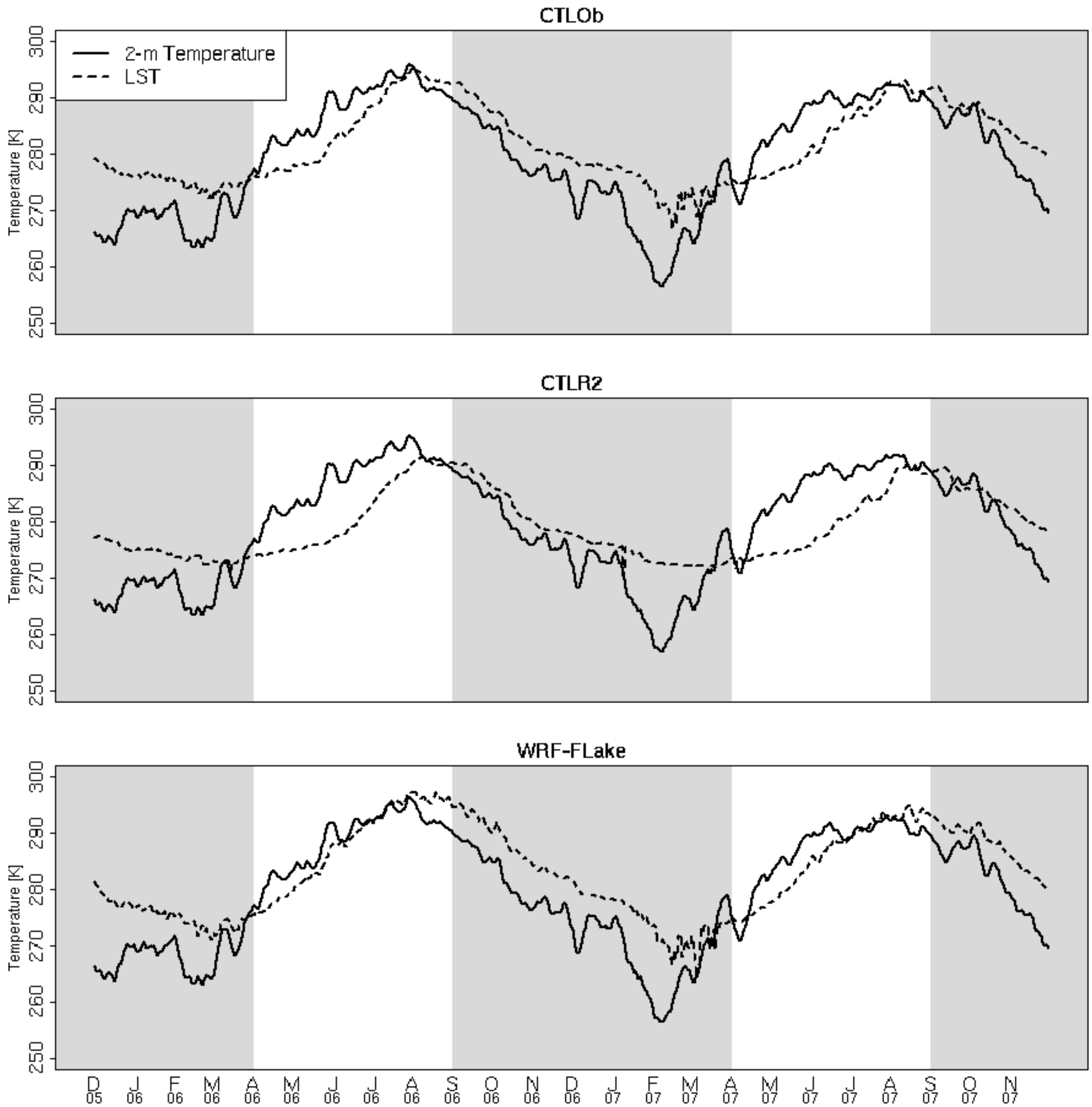

FIG. 9. Daily LSTs (dashed) and 2-m temperature (solid) averaged over the Great Lakes basin for CTLOb (top), CTLR2 (middle) and WRF-FLake (bottom). The air temperatures have a 10-point smoother applied to filter out short term variability. Gray shading denotes the climatological lake unstable season. Note that the use of smoothing, as well as temporal and spatial averaging, de-emphasizes differences between the air temperatures simulated by the three runs.